Acta Polytechnica CTU Proceedings **50**:36–43, 2024
https://doi.org/10.14311/APP.2024.50.0036

Published by the Czech Technical University in Prague

SUBSTRATE EFFECT IN THE EVALUATION OF ELASTIC MODULUS OF THIN PVD COATINGS FROM NANOINDENTATION

František Lofaj

Slovak Academy of Sciences, Institute of Materials Research, Watsonova 47, 040 01 Košice, Slovakia
correspondence: flofaj@saske.sk

Abstract. The comparison of nanoindentation results on reactive HiTUS TiZrHf+ME-N_y (ME = Nb, V, Ta and VNbTa) and reactive DCMS NbMoTaW coatings showed that the influence of substrate stiffness is still not fully eliminated in the evaluation of indentation modulus. To obtain comparable results by keeping the systematic error resulting from the existing evaluation procedures the same, nanoindentation should be performed using the same test parameters, a method for depth profile acquisition, a data evaluation procedure, and coatings with similar thicknesses on the same type of substrate. Applying these rules to nanoindentation on TiZrHf+ME-N_y coatings showed that the addition of ME = Nb, V, Ta, and VNbTa caused some degradation of mechanical properties indicating negligible or even negative "cocktail effect".

Keywords: Thin PVD films, nanoindentation, substrate effect elimination, multi-element nitride coatings.

1. Introduction

The nanoindentation testing on thin hard coating/softer substrate (and vice versa) systems always generates "composite" values due to simultaneous loading and response from the coating and substrate. The problem can be solved using several different approaches. Possibly the first way to extract coating hardness from the composite values and known as "10 % (relative depth) rule", was proposed by H. Bückle in 1959 [1]. It was suggested that the hardness values obtained from the relative depths below 10 % of the coating thickness should be used because the contribution from the substrate would still be very limited. Unfortunately, this rule fully corresponds to the H. L. Mencken quote: "For every complex problem there is an answer which is clear, simple and wrong" [2]. It is only a rule of thumb with limited applicability to hardness measurements and its use for the determination of an indentation modulus is principally not correct [3, 4]. The reason is that the size of the plastic field under the indenter defined by the yield stress can be confined only to the coating within the limited penetration depth range whereas the elastic field would extend into the substrate without any limit. Moreover, the stress field is affected by the ratio between elastic moduli of the coating and substrate and even by their interactions [5, 6]. Since the "10 % rule" is not able to reflect all these interactions, significant efforts were devoted to the refinement of the analysis of nanoindentation data from thin coatings. Starting from the early 1990s, various theoretical models have been developed to solve the problem of substrate effect analytically. The common features of these solutions were that they considered indentation as a deformation of coating and substrate in series and that they were fitted to experimentally obtain hardness and indentation modulus (relative) depth profiles. Depending on the physical processes obtained in the solutions, three groups of the models can be distinguished:

(1.) linear transition models involving the works of Jönsson&Hogmark [7], Burnett&Rickerby [8], Doerner&Nix [9], He&Li [10], Chicot&Lesage [11], Puchi-Cabrera [12], etc.;

(2.) energy models including works of Korsunsky&Bull [13, 14],

(3.) Gao's model & its modifications including studies of Gao&Chiu [15], Menčík [16], Song&Pharr [17], Hay&Crawford [5] etc.

Most of these models, were applicable only to the coating/substrate systems in which the elastic modulus of the coating was less than twice that of the substrate [5]. However, very stiff coatings can provide additional support against the deformation of the substrate. The additional and parallel influence of the coating on the substrate was introduced into the Song&Pharr's model [17] by Hay&Crawford (H&C) [5]. H&C model applies to the systems with $\leq$ 10-fold ratio between the elastic moduli of coating and substrate and the range of relative indentation depths (plateau width) available for the extrapolation to zero depth was expanded well above 10 % relative depth. The disadvantage is that the obtained indentation moduli are highly sensitive to the accuracy of the additional input parameters, especially Young's modulus of the substrate and coating thickness.

The results of theoretical works on nanoindentation in coating/substrate systems were reflected in the standardization efforts which were summarized in ISO 14577-4:2016 standard [18]. It prescribes that the true hardness and modulus of hard coatings on softer

Substrate	**Young's modulus** E **[GPa]**	**Poisson's ratio** ν **[–]**	$H_{IT\#}$ **[GPa]**	$E_{IT\#}$ **[GPa]**
(0001) sapphire	435 [25]	0.29 [25]	27.57 ± 0.27	458.7 ± 3.3
tempered 100Cr6 steel	210 (190–210) [26, 27]	0.285 (0.27–.30) [27]	9.25 ± 1.0	250.0 ± 9.5
(111) Si wafer	187 (186.5) [28]	0.223 (0.22–0.28) [28]	13.07 ± 0.13	193.6 ± 1.2
Ti6Al4V alloy	114 [29]	0.342 [29]	5.20 ± 0.16	133.2 ± 2.2

TABLE 1. Mechanical properties of the substrates used in the calculations (E and ν, and measured by nanoindentation in CSM mode (H_{IT} and E_{IT}).

substrates can be determined by the extrapolation of the values from the plateau at the maximum of the corresponding profile to zero penetration depth (load). It should be noted that such a procedure does not explicitly involve any analytical solution and the way the corresponding depth profile was obtained.

The simplest way to generate statistically reliable hardness and modulus depth profiles is to perform a sufficiently large number of individual loading/unloading tests until predefined depths in the range from less than 100 nm up to the depths approaching the coating thickness. Analogous depth profiles from the reduced number of indents can be obtained when several partial unloading/re-loadings are applied during the loading part of the loading/unloading tests. This mode is usually called "continuous multicycle" (CMC). Further advancement of CMC led to the "sinusoidal loading" or "continuous stiffness measurements" (CSM) [19–22] mode which involves an overlap of continuous sinusoidal load with small (constant absolute or constant relative) amplitude and conventional continuous loading. The advantage of CSM mode is a much higher speed of the generation of the corresponding depth profiles with better accuracy from a smaller number of indents. Statistical reliability of CSM tests is further improved due to the reduction of thermal drift and low-frequency noise effects [21]. The disadvantage of CSM mode is the contribution of "plasticity error" causing deviations at lower frequencies, especially in the materials with high E/H ratio [22]. It is related to small plastic deformation added to the elastic deformation due to a higher total load at the end of the cycle than at its beginning. However, plasticity error can be corrected [21] or significantly reduced using an appropriate combination of amplitude, frequency and loading rate [22]. It can be also eliminated when using the so-called Quasi-CSM (QCSM) mode when sinusoidal oscillations are applied only to repeated, short dwell-time periods during a continuous loading cycle [23].

Regardless of the method depth profiles were obtained, ISO standard procedure should be used to deduce the corresponding coating properties without the influence of the substrate. Sinusoidal modes (CSM and CSMTF) seem to be easier, faster and more precise than CMC and loading/unloading tests. Moreover, the ISO procedure is already built in the evaluation software of sinusoidal modes including that on the H&C model and known as "CSM for thin films" (CSMTF) mode. However, a comprehensive comparison of the evaluation of nanoindentation results considering different methods for depth profile generation, differences between conventional CSM and CSM treated based on the H&C model with the effect of substrate properties are still missing.

Therefore, the current work aimed to quantify the differences in the obtained hardness and moduli from the depth profiles obtained using different modes and on the coating/substrate systems with different substrate's Young's moduli on the statistically sufficient set of coatings. The work is the extension of our previous on 4 different substrates [24] from one up to six types of multi-transition metal-nitride ((TiZrHf+ME)-N_y, where ME = V, Nb, Ta and NbMoTaW-N_y) coatings with different stoichiometry spanning from pure metallic high entropy stabilized alloys ($y = 0$) up to stoichiometric nitrides ($y = 1$).

2. Materials and methods

2.1. Coating deposition

The studied coatings were deposited by sputtering on four different substrates from six different composite targets. The substrates involved polished single crystalline (111) Si and (0001) sapphire wafers, the polished discs of polycrystalline tempered 100Cr6 steel and Ti6Al4V alloy with different elastic moduli (see Table 1). The targets included TiZrHf, TiZrHfV, TiZrHfNb, TiZrHfTa, TiNbVTaZrHf and NbMoTaW discs with the diameters 76.2 mm and thicknesses of around 6.35 mm (Table 2).

The TiZrHf-based nitride coatings were produced by reactive High Target Utilization Sputtering (model S500, Plasma Quest Ltd., UK) from the above targets under the sputtering conditions optimized earlier [30] and applying different flows of nitrogen, x (in standard cubic centimeters per minute, sccm), into the sputtering Ar atmosphere (120 sccm). The values of x were usually in the range 0–10 sccm when stoichiometric composition was achieved. The structure and composition of these coatings were described earlier [30]. The metallic NbMoTaW coating was deposited using balanced DC magnetron sputtering at 300 W on a sapphire substrate heated to 500 °C at a floating bias.

Target	Ti [%]	Zr [%]	Hf [%]	Nb [%]	V [%]	Ta [%]	Mo [%]	W [%]
TiZrHf (99.6 %)#	33	33	34	–	–	–	–	–
TiZrHfV (>99.5 %)*	32	18	18	–	32	–	–	–
TiZrHfNb (>99.5 %)*	33	19	19	29				
TiZrHfTa (>99.5 %)*	33	19	19	–	–	29	–	–
TiNbVTaZrHf (>99.5 %)*	20	12	12	18	20	18	–	–
NbMoTaV (>99.9 %)*	–	–	–	25	–	25	25	25

*Testbourne, Ltd.; # Porexi

Table 2. The list of the targets and their nominal compositions used for the deposition of the studied nitride coatings.

2.2. Nanoindentation

Nanoindentation tests were performed with freshly calibrated Berkovich diamond tip in G 200 (Agilent/KLA, USA) nanoindenter under load control with the constant strain rate of $0.05\,s^{-1}$ using four techniques – loading/unloading, CMC, CSM and CSMTF. In both CSM cases, the frequency of 45 Hz and the amplitude of 2 nm were applied to reduce the contribution of plastic deformation during sinusoidal loading [22]. On each coating, two sets of 16 indents up to 600 (or 800) nm depth were carried out. The depth profiles were treated according to ISO 14577-4 with the lower limit of the plateau range of >80 nm determined by tip area calibration. The upper limit depended on the shape of the average depth profile and measurement mode: in the CSM case, the upper depth limit was often within 10 % of the relative coating thickness whereas when Hay&Crawford correction [5] was considered, it may exceed that depth due to improved consideration of substrate effect. The thicknesses of the coatings were measured using scanning electron microscopy (SEM, models Auriga Compact, Zeiss, Germany) on the fractured cross sections of the coatings deposited on Si wafers.

3. Results and Discussion

3.1. Depth profiles by different methods

To compare the depth profiles generated using four different methods, only one TiZrHfVNbTa-xN coating (x = 6 sccm N_2) with stoichiometric (y = 1) composition and thickness of 1700 nm on the silicon wafer was used. Figure 1a shows the depth profile of the indentation modulus obtained using simple loading/unloading tests. Each value calculated using Oliver&Pharr (O&P) method corresponds to the average from 10 indents and 9 different depths were employed to obtain the profile. The data were valid in the range above 80 nm. The extrapolation procedure from the plateau-like region from 80 nm up to 200 nm resulted in the indentation modulus, E_{IT} = 295 ± 35 GPa whereas the "10 % rule" approach gave around 284 GPa. The hardness values, H_{IT} = 29.5 ± 2 GPa were identical in both cases.

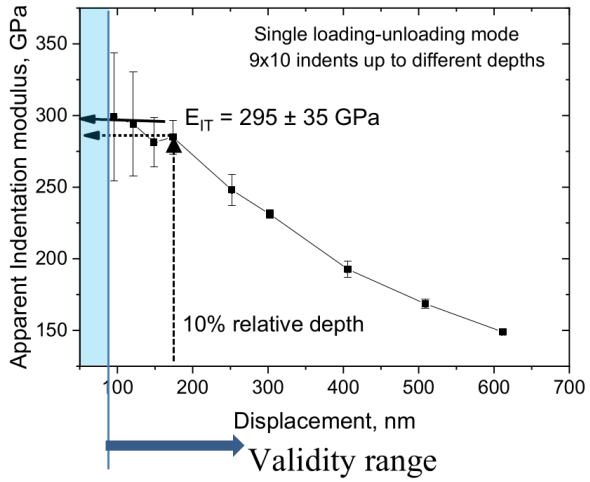

(a).

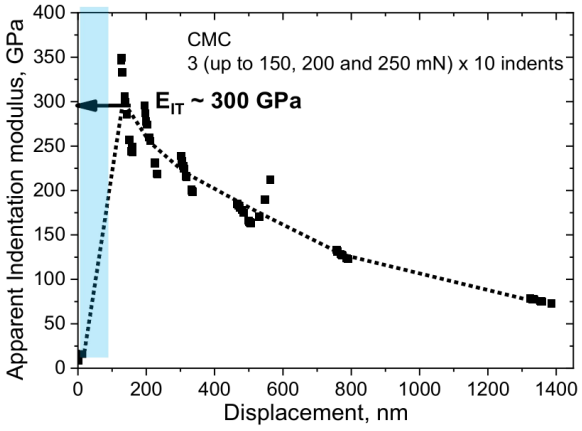

(b).

Figure 1. Indentation modulus depth profiles obtained on TiZrHfVNbTa-xN coating (x = 6 sccm N_2) on (111) silicon substrate using (A) – 90 simple loading/unloading tests; (B) – 30 tests with 6 partial unloadings in each test. The zone below 80 nm should not be considered due to indenter tip surface area calibration effects.

Method	E_{IT} [GPa] ISO	E_{IT} [GPa] 10 % rule	H_{IT} [GPa] ISO	H_{IT} [GPa] 10 % rule
loading/unloading	295 ± 35	~285	29.5 ± 2.0	29.5
CMC	~300	(~300)	~28	~28
CSM	290 ± 15	~270–275	27.2 ± 2.6	27.2
CSM+H&C (CSMTF)	275 ± 15	~250	28.2 ± 2.7	28.2

TABLE 3. Summary of the indentation modulus and hardness values calculated using ISO and the "10 % rule" procedures from the depth profiles by four different methods on 1700 nm thick TiZrHfVNbTa-xN coating (x = 6 sccm N_2) deposited on (111) silicon substrate by reactive HiTUS.

In the case of CMC tests (Figure 1b), 10 indents up to 100 mN, 200 mN and 250 mN loads with 6 partial unloading in each test were performed. Each unloading was evaluated according to O&P method but the averaging was not performed due to variations in the depths during unloadings within each test. It resulted in relatively large scatter of the data and only rough estimate of the coating properties. The approximate indentation modulus was around 300 GPa and hardness was 28 GPa. Possible differences between extrapolation according to ISO standard and the "10 % rule" were not observed due to excessive scatter of the data.

In the case of CSM tests (Figure 2a), the average depth profile curve was smooth and large scatter was present only below 100 nm depths. The maximum at 100 nm was followed by a smooth decrease without a clear plateau. The calculation of the corresponding E_{IT} depends on subjectively selected depth range limits. In the range from 100 nm to 150 nm, E_{IT} = 290 ± 15 GPa whereas only around 275 GPa were obtained using the "10 % rule" approach. The hardness profile exhibited a well-defined plateau up to 250 nm depth. Therefore, the same values of H_{IT} of 27.2 ± 2.6 GPa were obtained when applying ISO and the "10 % rule" procedure. Figure 2b illustrates the effect of the correction on substrate modulus and coating thickness included in H&C correction (CSMTF) on the modulus depth profile compared to the standard CSM profile. The differences are visible already in the 100–150 nm ("plateau") depth region and increase with the increase of penetration depth. Subsequently, different indentation moduli (full arrows) were obtained from these regions in CSM (~275 GPa) and CSMTF (~263 GPa). The average values from 9 indents (after removal of the outcasts) based on ISO procedure resulted in the average E_{IT} = 275 ± 15 GPa. At 10 % relative depth, the values were ~270 GPa and ~250 GPa, respectively. The hardness profile is not affected by the correction and it was H_{IT} = 28.2 ± 2.7 GPa.

Table 3 compares the results of nanoindentation tests using four different methods for depth profiles and evaluated using ISO and the "10 % rule" procedure. It should be emphasized that the results were obtained on the same and relatively thick (1700 nm) coating on silicon substrate, which eliminated possible effects of variations between coatings, substrates and

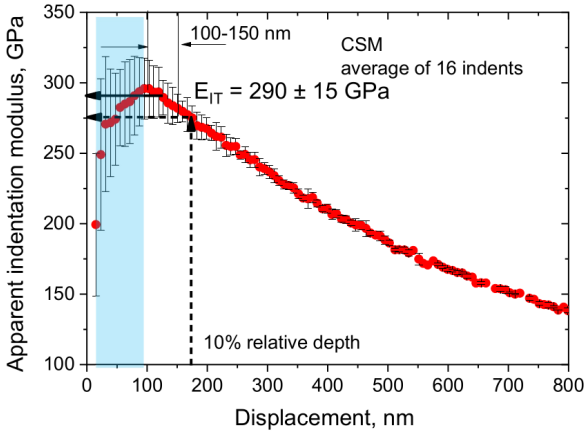

(A).

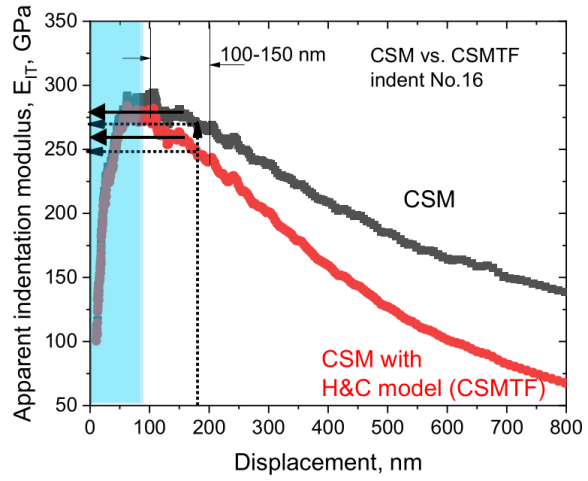

(B).

FIGURE 2. An average (from ≤16 indents) indentation modulus depth profiles on TiZrHfVNbTa-xN coating (x = 6 sccm N_2) on (111) silicon substrate using (A) – continuous stiffness measurements (CSM) tests; (B) – the comparison of E_{IT}) depth profiles from 1 indentation test using CSM and CSM with the correction on substrate properties based on Hay&Crawford model (CSMTF).

small thickness. The values of E_{IT} (and H_{IT}) calculated according to ISO standard from the profiles obtained by different methods varied from 275 GPa to 300 GPa (and 27.2 GPa to 29.5 GPa), which was within the scatter of each measurement. Thus, all four methods are suitable for the determination of hardness and modulus profiles in coating/substrate systems. However, CSM-based methods are experimentally easier, faster, more effective and conservative, especially with the correction on substrate properties. The differences between E_{IT} values calculated according to ISO and the "10 % rule" procedures were also not very large and fully overlapped in H_{IT}. However, it does not rehabilitate the "10 % rule" approach because the coating was relatively thick which could shield the substrate and prevent the collision of the calculation range with the lower limit of validity range. Therefore, additional measurements on thinner coatings were performed.

3.2. Coating thickness effect

Analogous nanoindentation tests using CSM only were performed on the NbMoTaW coating with a thickness of 610 nm deposited using DC magnetron sputtering on (0001) sapphire substrate. Figure 3 compares the indentation modulus and hardness depth profiles in CSM and corrected CSM (CSMTF). The H&C correction introduced a reduction of the indentation modulus profile and plateau became more pronounced than in the case of CSM. It caused that the modulus could be calculated from the relative depth range from 16 % to almost 30 % which is well above 10 % of the relative depth. The resulting value from CSM was higher by 35 GPa than that (354 ± 11 GPa) obtained from the corrected CSM profile. The calculation employing the "10 % rule" completely failed: the depth of 61 nm falls into the range where the tip-blunting effects are dominant and the data are invalid. The hardness profile from CSM (Figure 3b) was not affected by the correction and it was H_{IT} = 30.7 ± 1.0 GPa. Applying the "10 % rule" to hardness also failed because of the same reason. Thus, Figure 3 even more clearly than the data in Table 3 demonstrates why the "10 % rule" approach should be avoided in the determination of the mechanical properties of thin coatings from nanoindentation.

3.3. The effect of substrate modulus

This study involved one stoichiometric TiZrHfVNbTa-xN coating approximately 1325 nm thick deposited by reactive HiTUS at x = 6 sccm N_2 flow simultaneously on four different substrates listed in Table 1. Two measurements were performed using independently CSM and corrected CSM (CSMTF) methods on each substrate. The results summarized in Figure 4a indicate that E_{IT} and H_{IT} values from both measurements were within the scatter and they are reproducible. Besides that, systematic and substantial differences in the 20–50 GPa range between apparent E_{IT} values

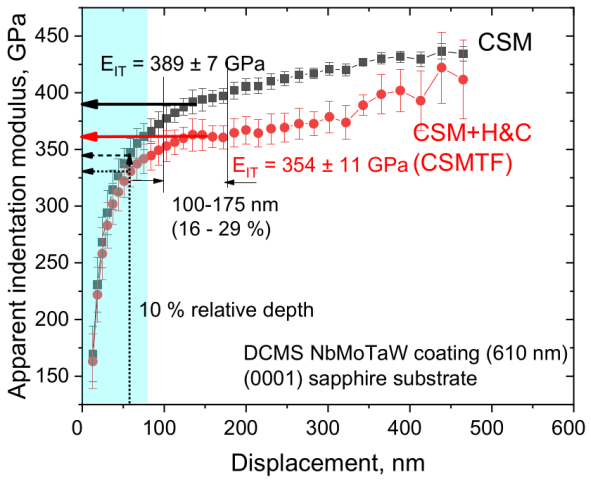

(A).

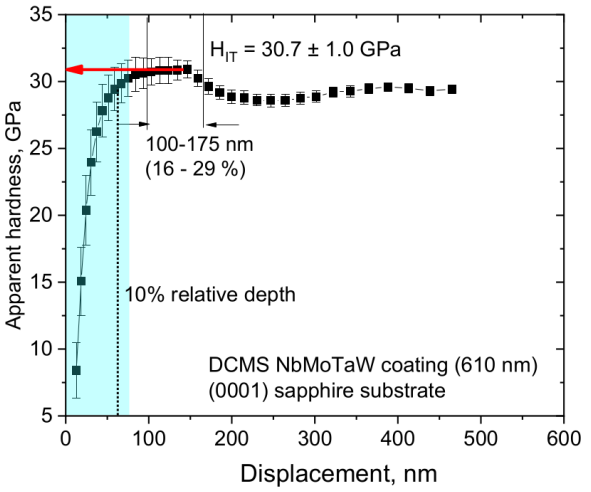

(B).

Figure 3. Depth profiles of (A) – indentation modulus, (B) – hardness, obtained using CSM method during nanoindentation of 610 nm thin r-DCMS NbMoTaW coating.

from CSM and corrected CSM (CSMTF) and in the 65–150 GPa range the increase of the substrate modulus from Ti-alloy to sapphire. Thus, the influence of the substrate elastic modulus on the coating modulus evaluation was not fully eliminated both in CSM and in the H&C-modified CSM and its further refinement is necessary. On the contrary, hardness (Figure 4b) varied only from 27 GPa to 36 GPa with an average value of around 31.5 GPa and the differences were mostly within the scatter of individual measurements.

3.4. Best practice recommendations

The above results suggest that substrate influence in the evaluation of indentation modulus is still not fully eliminated and the current solutions, despite the incorporation of ISO 14577-4 procedure, generate systematic differences exceeding measurement scatter. In the case of the presence of systematic errors, the following rules can be recommended to produce

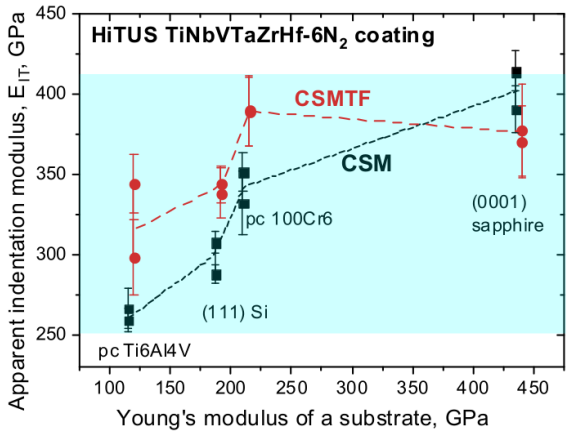

(A).

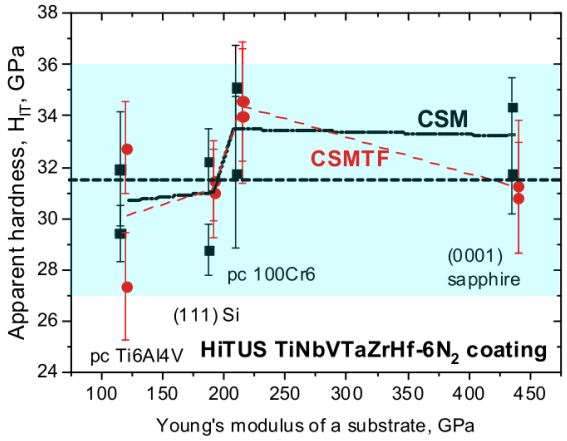

(B).

FIGURE 4. The effect of substrate modulus on the calculated values of indentation modulus – (A), and hardness – (B), in CSM and independent corrected CSM (CSMTF) models. The data from CSMTF were intentionally offset for better visibility [24].

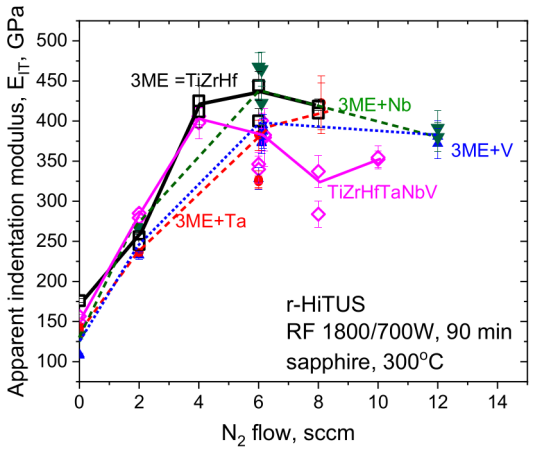

(A).

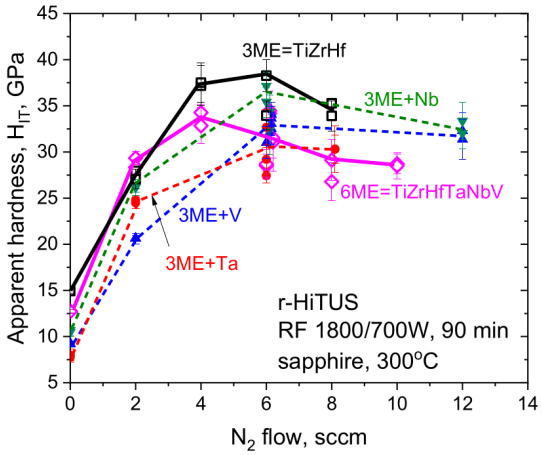

(B).

FIGURE 5. The dependences indentation modulus – (A), and hardness – (B), in TiZrHf+ME-N_y (ME = V, Nb, Ta) on the flow of nitrogen added in the sputtering Ar atmosphere (and subsequently, stoichiometry, y) during reactive HiTUS deposition.

comparable values of indentation modulus in thin coating/substrate systems:

- strictly follow ISO 24577-4 and principally avoid the "10 % rule" despite its simplicity and small bias in hardness determination in sufficiently thick coatings;
- use sharp tip and frequent tip area calibration to minimize the depth range in which the results are dominated by tip bluntness [31];
- the coatings with a thickness >1 µm are preferred; reliable results from thinner coatings require very sharp tips and better consideration of substrate effects;
- use the same method for obtaining corresponding depth profiles (the CSM method with the optimized parameters seems to be suitable);
- use the same evaluation method (Hay&Crawford correction brings some benefits but it is sensitive to substrate modulus and coating thickness. Moreover, the results may not be directly comparable with the earlier data);
- use the same substrates with the well-defined elastic modulus;
- at least two independent nanoindentation measurements should be performed on each coating to take into consideration coating uniformity as well as measurement accuracy and repeatability.

3.5. Application to measurement in TiZrHfVNbTa-xN coatings

The recommendations from Section 3.4 were applied in the measurements and evaluation of the effect of V, Nb, Ta and nitrogen additions on mechanical properties of TiZrHf-ME-N_y coatings. It should be emphasized that although only the sapphire substrates and CSMTF method were employed to keep possible systematic errors the same, the resulting values are only relative and should be used only for comparison. The full lines in Figures 5a and 5b indicate the de-

pendences in the reference TiZrHf-N_y (ME = 0) and TiZrHfVNbTa-N_y (ME = VNbTa) coatings, respectively, as a function of nitrogen flow. The broken lines correspond to TiZrHf+ME-N_y. The highest values in all systems were above certain critical flow of nitrogen which was around 6 sccm N_2 when stoichiometry was achieved [30]. The curves in TiZrHf-N_y coatings were above all other curves and also the maximum E_{IT} = 490 GPa and H_{IT} = 39 GPa were obtained in this system. Despite limited reliability of the absolute values, good agreement with the properties reported for similar multi-transition metal nitrides produced by reactive DC magnetron sputtering [32] was obtained. The relative comparison indicates that the additions of ME = V, Nb, Ta and VNbTa caused small degradation of H_{IT} and E_{IT} which became more visible at higher nitrogen flows. The smallest degradation seems to be in the coatings with ME = Nb whereas it is the most pronounced in TiZrHfVNbTa-N system. Thus, the "cocktail effect" resulting from the additions of additional elements considered in the high entropy alloys, seems to be negligible or might be even negative in TiZrHf-ME-N_y coatings.

4. Conclusions

The results of the current study suggest that the influence of substrate stiffness is still not fully eliminated in the evaluation of indentation modulus which causes systematic differences exceeding measurement scatter between coatings deposited on sufficiently different substrates (without consideration of substrate influence on coating growth and structure). To keep the systematic error the same and to obtain comparable relative results, nanoindentation should be performed using the same test parameters, method for depth profile acquisition, data evaluation procedure and coatings with similar thicknesses on the same type of substrate. The application of these rules to nanoindentation on TiZrHf+ME-N_y coatings deposited by reactive HiTUS showed that the addition of ME = V, Nb, Ta and VNbTa caused some degradation of mechanical properties indicating negligible or even negative "cocktail effect".

Acknowledgements

This work was supported by the Slovak Academy of Sciences via the International Visegrad Fund (project JP39421 of V4-Japan Joint Research Program) and Slovak Research and Development Agency (project APVV 21-0042).

References

[1] H. Bückle. Progress in micro-indentation hardness testing. *Metallurgical Reviews* **4**(1):49–100, 1959. https://doi.org/10.1179/095066059790421746

[2] H. L. Mencken Quotes. [2024-08-28]. https://www.brainyquote.com/authors/h-l-mencken-quotes

[3] A. C. Fischer-Cripps. *Nanoindentation*. Springer, New York, 2004. Second printing.

[4] S. Zak, C. O. W. Trost, P. Kreiml, M. J. Cordill. Accurate measurement of thin film mechanical properties using nanoindentation. *Journal of Materials Research* **37**(7):1373–1389, 2022. https://doi.org/10.1557/s43578-022-00541-1

[5] J. Hay, B. Crawford. Measuring substrate-independent modulus of thin films. *Journal of Materials Research* **26**:727–738, 2011. https://doi.org/10.1557/jmr.2011.8

[6] A. Lassnig, S. Zak. Precise determination of Young's modulus of amorphous CuZr/nanocrystalline Cu multilayer via nanoindentation. *Journal of Materials Research* **38**:3324–3335, 2023. https://doi.org/10.1557/s43578-023-01057-y

[7] B. Jönsson, S. Hogmark. Hardness measurements of thin films. *Thin Solid Films* **114**(3):257–269, 1984. https://doi.org/10.1016/0040-6090(84)90123-8

[8] P. J. Burnett, D. S. Rickerby. The mechanical properties of wear-resistant coatings: I: Modelling of hardness behaviour. *Thin Solid Films* **148**(1):41–50, 1987. https://doi.org/10.1016/0040-6090(87)90119-2

[9] M. F. Doerner, W. D. Nix. A method for interpreting the data from depth-sensing indentation instruments. *Journal of Materials Research* **1**(4):601–609, 1986. https://doi.org/10.1557/JMR.1986.0601

[10] J. L. He, W. Z. Li, H. D. Li. Hardness measurement of thin films: Separation from composite hardness. *Applied Physics Letters* **69**(10):1402–1404, 1996. https://doi.org/10.1063/1.117595

[11] D. Chicot, J. Lesage. Absolute hardness of films and coatings. *Thin Solid Films* **254**(1-2):123–130, 1995. https://doi.org/10.1016/0040-6090(94)06239-H

[12] E. S. Puchi-Cabrera. A new model for the computation of the composite hardness of coated systems. *Surface and Coatings Technology* **160**(2):177–186, 2002. https://doi.org/10.1016/S0257-8972(02)00394-8

[13] S. J. Bull. A simple method for the assessment of the contact modulus for coated systems. *Philosophical Magazine* **95**(16-18):1907–1927, 2015. https://doi.org/10.1080/14786435.2014.909612

[14] A. M. Korsunsky, M. R. McGurk, S. J. Bull, T. F. Page. On the hardness of coated systems. *Surface and Coatings Technology* **99**(1):171–183, 1998. https://doi.org/10.1016/S0257-8972(97)00522-7

[15] G. Huajian, C. Cheng-Hsin, L. Jin. Elastic contact versus indentation modeling of multi-layered materials. *International Journal of Solids and Structures* **29**(20):2471–2492, 1992. https://doi.org/10.1016/0020-7683(92)90004-D

[16] J. Menčík, D. Munz, E. Quandt, et al. Determination of elastic modulus of thin layers using nanoindentation. *Journal of Materials Research* **12**(9):2475–2484, 1997. https://doi.org/10.1557/JMR.1997.0327

[17] A. Rar, H. Song, G. M. Pharr. Assessment of new relation for the elastic compliance of a film-substrate system. *MRS Online Proceedings Library* **695**:10101, 2001. https://doi.org/10.1557/PROC-695-L10.10.1

[18] ISO 14577-4:2016 Metallic materials: instrumented indentation test for hardness and material parameters – Part 4: Test method for metallic and non-metallic coatings, 2016.

[19] W. C. Oliver, J. B. Pethica. Method for continuous determination of the elastic stiffness of contact between two bodies. U.S. Patent 4 848 141, 18 July 1989.

[20] J. Hay, P. Agee, E. Herbert. Continuous stiffness measurement during instrumented indentation testing. *Experimental Techniques* **34**:86–94, 2010. https://doi.org/10.1111/j.1747-1567.2010.00618.x

[21] P. S. Phani, W. C. Oliver, G. M. Pharr. Measurement of hardness and elastic modulus by load and depth sensing indentation: Improvements to the technique based on continuous stiffness measurement. *Journal of Materials Research* **36**(11):2137–2153, 2021. https://doi.org/10.1557/s43578-021-00131-7

[22] B. Merle, V. Maier-Kiener, G. M. Pharr. Influence of modulus-to-hardness ratio and harmonic parameters on continuous stiffness measurement during nanoindentation. *Acta Materialia* **134**:167–176, 2017. https://doi.org/10.1016/j.actamat.2017.05.036

[23] L. Lorenz, T. Chudoba, S. Makowski, et al. Indentation modulus extrapolation and thickness estimation of ta-C coatings from nanoindentation. *Journal of Materials Science* **56**:18740–18748, 2021. https://doi.org/10.1007/s10853-021-06448-2

[24] F. Lofaj, T. Csanádi, L. Kvetková, et al. Micromechanical properties of reactive HiTUS TiNbVTaZrHf–N coatings on different substrates. *Powder Metallurgy Progress* **22**(1):31–42, 2022. https://doi.org/10.2478/pmp-2022-0005

[25] Valley Design Corp. Properties of sapphire substrate and sapphire wafers. [2024-09-06]. https://valleydesign.com/sappprop/

[26] MatWeb. [2024-09-06]. https://www.matweb.com/search/datasheet.aspx?matguid=d0b0a51bff894778a97f5b72e7317d85&ckck=1

[27] ASTM 52100 Bearing Steel. [2024-09-06]. https://www.astmsteel.com/product/52100-bearing-steel-aisi/

[28] UniversityWafer. What are the mechanical properties of monocrystalline silicon? [2024-09-06]. https://www.universitywafer.com/mechanical-properties-monocrystalline-silicon.html

[29] True Geometry. Mechanical properties of titanium Grade 5: A comprehensive review. [2024-09-06]. https://blog.truegeometry.com/designs3D/Titanium_Grade_5_Metal20240605.html

[30] F. Lofaj, L. Kvetková, T. Roch, et al. Reactive HiTUS TiNbVTaZrHf-N_x coatings: Structure, composition and mechanical properties. *Materials* **16**(2):563, 2023. https://doi.org/10.3390/ma16020563

[31] F. Lofaj, D. Németh. The effects of tip sharpness and coating thickness on nanoindentation measurements in hard coatings on softer substrates by FEM. *Thin Solid Films* **644**:173–181, 2017. https://doi.org/10.1016/j.tsf.2017.09.051

[32] A. Kirnbauer, A. Kretschmer, C. M. Koller, et al. Mechanical properties and thermal stability of reactively sputtered multi-principal-metal Hf-Ta-Ti-V-Zr nitrides. *Surface and Coatings Technology* **389**:125674, 2020. https://doi.org/10.1016/j.surfcoat.2020.125674